JOURNAL OF PLANKTON RESEARCH | VOLUME 27 | NUMBER 5 | PAGES 473–483 | 2005

Size dependence of coastal phytoplankton photosynthesis under vertical mixing conditions

PEDRO CERMEÑO[1]*, EMILIO MARAÑÓN[1,2], JAIME RODRÍGUEZ[3] AND EMILIO FERNÁNDEZ[1]

[1]DEPARTAMENTO DE ECOLOGÍA Y BIOLOGÍA ANIMAL, FACULTAD DE CIENCIAS DEL MAR, UNIVERSIDAD DE VIGO, 36310 VIGO, SPAIN, [2]LABORATOIRE D'OCÉANOGRAPHIE DE VILLEFRANCHE, CNRS-UPMC, 06234 VILLEFRANCHE-SUR-MER, FRANCE AND [3]DEPARTAMENTO DE ECOLOGÍA Y GEOLOGÍA, UNIVERSIDAD DE MÁLAGA, CAMPUS DE TEATINOS, 29071 MÁLAGA, SPAIN

*CORRESPONDING AUTHOR: pca@uvigo.es

Received February 2, 2005; accepted in principle March 24, 2005; accepted for publication April 6, 2005; published online April 18, 2005

Communicating editor: K.J. Flynn

We have determined the relationship between carbon-specific photosynthesis and phytoplankton cell size in a coastal ecosystem. The normalized size spectra of carbon (C) biomass and photosynthesis allow to determine both biomass and photosynthesis within any size class along the community size spectrum. By dividing the size spectra of photosynthesis and biomass, the size spectrum of C-specific photosynthesis is derived. Our results indicated a high variability in the slope of the C-specific photosynthesis size spectrum. Under favourable conditions for growth, in the upper euphotic layer, the slope was positive, indicating that larger phytoplankton attained higher C-specific photosynthesis rates than the smaller cells. This pattern represents a significant departure from the expected, literature value of −0.25 for the size-scaling of biomass-specific metabolism. We suggest that this change in the slope may be caused by the changes in the taxonomic composition along the community size spectrum. Towards the bottom of the euphotic layer, we observed a decrease in the slope of the C-specific photosynthesis size spectrum, which could be associated with an enhanced package effect in larger cells under light-limited conditions. These results question the applicability of single and overall exponents to describe the size scaling of photosynthesis in natural phytoplankton assemblages.

INTRODUCTION

From unicellular organisms to large mammals, size dependent metabolic rates conform to a power equation, $M = aW^b$, where M is the individual metabolic rate, W is organism size (biovolume or mass), a is the rate coefficient and b is the size scaling parameter, which usually takes a constant value of 3/4 for individual metabolic rates (i.e. −1/4 for biomass-specific metabolic rates) (Hemmingsen, 1960; Fenchel, 1974; Peters, 1983). The size scaling parameter represents metabolic constraints imposed by organism size and consequently is considered to determine how the energy flows through the community size spectrum (Platt *et al.*, 1984; Nielsen and Sand-Jensen, 1990; Rodríguez, 1994).

Theoretical models and empirical evidence suggest that, in marine pelagic ecosystems, the size distribution of living biomass within logarithmic size intervals follows a power function with a slightly negative exponent (Platt and Denman, 1978; Rodríguez and Mullin, 1986). Typically, the size structure of plankton communities is represented as a normalized size spectrum which is obtained by dividing the biomass in each logarithmic size interval by the width of that interval. This makes the biomass size distribution independent of the size intervals and thus more amenable to mathematical manipulation (Platt and Denman, 1978; Rodríguez and Mullin, 1986). For example, the normalized spectrum can be integrated over size, and the area under the model equation represents the total biomass. Taking into account the size-dependence of metabolic rates, Platt *et al.* (Platt *et al.*, 1984) developed a theoretical continuous model which, by using the normalized biomass spectrum, allows a quantification of the continuous flux of matter or energy through the pelagic

doi:10.1093/plankt/fbi021, available online at www.plankt.oxfordjournals.org

ecosystem. For instance, Blanco *et al.* (Blanco *et al.*, 1998) estimated zooplankton respiration using biomass size spectra and allometric relations and compared their estimates with measured data. They obtained a good correlation but highlighted that variability in allometric parameters may have an important effect on the resulting estimates. Further models have subsequently been developed which capture not only physiological processes but also ecological or environmental phenomena (Thiebaux and Dickie, 1993; Duplisea and Kerr, 1995).

Traditionally, all these models have used a constant size scaling exponent for metabolic rates (typically −0.25 for mass-specific metabolic rate). However, changes in this parameter could significantly alter both the estimated community metabolism and the relative contribution of each size category. A large body of empirical evidence suggests that the size dependence of specific growth rate may deviate significantly from the commonly used −0.25 power relationship as a result of suboptimal growth conditions and/or variability among specific groups such as diatoms and dinoflagellates (Schlesinger *et al.*, 1981; Banse, 1982; Blasco *et al.*, 1982; Sommer, 1989; Tang, 1995). In addition, a recent analysis of the relationship between phytoplankton photosynthesis and cell size under light-limited conditions predicts a significant decrease in the size scaling exponent of phytoplankton photosynthesis, as a result of trade-offs between intracellular pigment content and light harvesting efficiency (Finkel, 2001; Finkel *et al.*, 2004).

The community metabolism can also be approached by using the normalized metabolism spectrum, in which the normalized parameter is a metabolic rate (Quiñones, 1992, 1994a). Similarly to the biomass spectrum, the metabolism spectrum allows to estimate the total metabolism of organisms within any given size class, by integrating its normalized spectrum. Then, using the normalized spectra, it is possible to relate metabolism and biomass within any given size interval. This allows determination of the biomass-specific metabolic rate across the size spectrum, and thus to test the applicability of the size scaling metabolic relationships under natural conditions. Unfortunately, a prerequisite for the application of these models is the existence of regularities (i.e. good fitting of the $\log_2$-transformed data to a continuous linear model) along the community size spectra, which are subjected not only to physiological scaling factors but also to ecological ones (Dickie *et al.*, 1987). For plankton communities, regularities in the biomass spectrum have been established in open ocean ecosystems (Rodríguez and Mullin, 1986; Quiñones *et al.*, 2003). In contrast, coastal and freshwater ecosystems tend to show irregular biomass distributions, which reflect ecological factors affecting the size structure of the plankton community (Sprules and Munawar, 1986; Rodríguez *et al.*, 1987; Gasol *et al.*, 1991). Similarly, Quiñones (Quiñones, 1992), measuring size-fractionated respiration rates, found regularities in the metabolism spectra in steady-state open ocean environments. On the other hand, Quiñones *et al.* (Quiñones *et al.*, 1994b) observed irregularities in the metabolism spectra at a frontal station in the Alboran Sea (Mediterranean Sea), an area characterized by a very active mesoscale circulation.

For this study, we took into account the above mentioned issues, and only those samples showing regularities were used. In essence, our data set was obtained from nutrient-replete samples collected under vertical mixing conditions. The sampling was carried out in a coastal embayment (Ría de Vigo, northwestern Iberian Peninsula) that is characterized during winter by continuous vertical mixing (Álvarez-Salgado *et al.*, 2003). Our main goal was to determine the size scaling exponent of phytoplankton photosynthesis in high-nutrient conditions and along a sharp, vertical light gradient. Our observations allowed us to confirm the high variability of this parameter, which seems to depend on the taxonomic variability along the community size spectrum.

METHOD

Sampling

A total of five visits to a central station in the Ría de Vigo (42°14.09′ N, 8°47.18′ W) were carried out from November 2001 to March 2002. On each visit, we recorded vertical profiles (0–40 m) of temperature and conductivity with a SeaBird Electronics 25 CTD probe. The vertical distribution of photosynthetically active irradiance (PAR, 400–700 nm) was measured with a spherical quantum sensor connected to a LiCor datalogger. Seawater samples for chemical and biological measurements were collected using single 5-L Niskin bottles. Samples for the analysis of dissolved inorganic nutrients (nitrate, nitrite, silicate, phosphate and ammonium) were obtained from 0, 5, 10, 15, 20 and 30 m. These samples were immediately frozen and stored at −20°C until they were analysed in the laboratory following the methods described in Grasshoff *et al.* (Grasshoff *et al.*, 1999).

Size-fractionated chlorophyll *a* and biomass size spectra

For the determination of size-fractionated chlorophyll *a* (Chl *a*) concentration, two replicates of 250-ml samples were filtered sequentially through 20-, 5-, 2- and 0.2-μm polycarbonate filters, using low-vacuum pressure (<100 mm Hg). Filters were stored frozen at −80°C until further analysis, which took place within 4 months of sampling. Pigment extraction was carried out by placing the filters in 90% acetone during 12 h. Chl *a* concentration was deter-

mined fluorimetrically using a TD-700 fluorometer which had been calibrated with pure Chl *a* (Sigma).

We obtained estimates of cell size and abundance of pico- and small nanophytoplankton (0.2–5 μm equivalent spherical diameter, ESD) by using flow cytometry, on the basis of the fluorescence signals and forward- and side-light scatter (FSC and SSC respectively). Following the recommendation of Vaulot *et al.* (Vaulot *et al.*, 1989), 10-ml samples were preserved with glutaraldehyde (1% v/v) and stored in liquid nitrogen until further analysis, which took place within 2–3 weeks. In the laboratory, flow cytometry samples were analysed with a FACScan (Becton Dickinson) flow cytometer following protocols described in Rodríguez *et al.* (Rodríguez *et al.*, 1998). For the analysis of larger cells under the microscope, 100-ml samples were preserved with Lugol's solution. After sedimentation of a subsample (10–25 ml), cells were counted and measured at ×100 and ×200 on a Leitz Fluovert inverted microscope connected to a VIDS IV (Analytical Measuring Systems) image analysis system. Cell volume was estimated assuming an ellipsoidal shape (Ruiz *et al.*, 1996). Analytical subranges for flow cytometry and image analysis were ~0.7–10 μm ESD and 5–70 μm ESD, respectively. Flow cytometry and microscopy image analysis analytical subranges were coupled in order to obtain a size-abundance spectrum of the whole autotrophic plankton community, from small cyanobacteria to large dinoflagellates and diatoms (Rodríguez *et al.*, 1998, 2002). Finally, cell carbon biomass was estimated by applying empirical volume to carbon conversion factors (Verity *et al.*, 1992). Biomass for each size category was then calculated by multiplying cell abundance by cell carbon, thus generating size spectra of carbon biomass. It is conceivable that the different methodologies (i. e. preservative agents) used for each size range biased our estimates of phytoplankton abundance and cell size. If any consistent effect had differentially affected these estimates, it would have been detected in the coupling of both analytical subranges, resulting in a mismatch between the two types of spectra. However, we consistently obtained a smooth transition between both analytical subranges resulting in continuous size spectra from picoplankton to microplankton. These results gave us reassurance on the validity of our estimates of abundance and cell size despite different analytical approaches.

Flow cytometry and image analysis allowed us to define different analytical populations which were related to different microalgal groups. Using flow cytometry we defined *Synechococcus* sp., cytometry population 1 (picoeukaryotes), cytometry population 2 (mainly nanoflagellates) and Cryptophytes. Image analysis allowed us to identify diatoms and other phytoplankters.

Size-fractionated photosynthesis

Size-fractionated photosynthetic rates were determined by the ^{14}C technique as detailed by Marañón *et al.* (Marañón *et al.*, 2004). Four 75-ml acid-cleaned polystyrene bottles (three transparent and one dark bottle) were filled with seawater from surface, 10 and 20 m depth. Each bottle was inoculated with ~370 kBq (10 μCi) of $NaH^{14}CO_3$ and incubated for 2 h starting at noon. We used an incubator that reproduced the irradiance conditions at the original depths where the samples had been collected. Temperature inside the incubator was kept within ±1.5°C of the original temperature at each sampling depth. At the end of the incubations, samples were sequentially filtered through 20-, 5-, 2- and 0.2-μm polycarbonate filters under low-vacuum pressure (<100 mm Hg). Inorganic carbon on the filters was removed by exposing them to concentrated HCl fumes overnight. Finally, the radioactivity on each sample was determined on a 1409–012 Wallac scintillation counter which used an internal standard for quenching correction.

Normalized size spectra and model formulation

In order to construct the normalized size spectrum of biomass, raw biomass data in each size class, [$b(v)$, in units of μg C L^{-1}], were divided by the size class width (Δv, in units of μm^3 per cell). As size classes are in logarithmic progression our resulting data set conformed to a power equation:

$$B(v) = \frac{b(v)}{\Delta v} = mV^r \qquad (1)$$

Similarly, the normalized size spectrum of metabolism was obtained from measurements of size-fractionated photosynthesis, [$p(v)$, in units of μg C L^{-1} h^{-1}]:

$$P(v) = \frac{p(v)}{\Delta v} = nV^s \qquad (2)$$

In these equations, V is the nominal size class (in units of μm^3 per cell) defined as the average point of the size class (see Blanco *et al.*, 1994), m and n are proportionality coefficients [in units of $(\mu m^3)^{-r}$ μg C $(\mu m^3\ L)^{-1}$ and $(\mu m^3)^{-s}$ μg C $(\mu m^3\ L\ h)^{-1}$], then $B(v)$ and $P(v)$ have units of μg C $(\mu m^3\ L)^{-1}$ and μg C $(\mu m^3 L\ h)^{-1}$, respectively. The parameters r and s are the power exponents of the corresponding equations. The lower and upper limits of the metabolism spectrum were defined taking into account the original limits of the biomass spectra (in our study from 0.9 to 70 μm ESD). Once calculated, $B(v)$ and $P(v)$ were $\log_2$-transformed and plotted against

$\log_2$-nominal size class (i.e. octave scale increase), which yielded the following linear functions:

$$\log_2 B(v) = m + r \,.\, \log_2 V$$

$$\log_2 P(v) = n + s \,.\, \log_2 V$$

In both instances, regression analysis was carried out using ordinary least squares linear regression. The lower limit of the biomass spectrum was defined as the size class with the maximum normalized biomass, thus neglecting the biomass data which represent the left side, normally distributed populations of the smallest phytoplankton cells. The determination coefficient (r^2) indicates the regularity of the spectrum, whereas the slope of the equation serves as an indicator of the size structure of the phytoplankton community in terms of biomass or photosynthesis. Figure 1 shows an example of normalized size spectra of biomass and photosynthesis obtained during this study.

Integration of the power equations (1) and (2) over V allowed us to calculate, respectively, carbon biomass and photosynthesis in any size range defined over the spectrum:

$$B(v) = \int m V^r d(v) \tag{3}$$

$$P(v) = \int n V^s d(v) \tag{4}$$

Equations (3) and (4) were then combined to determine the carbon-specific photosynthesis (P^{b}, in units of h^{-1}) as follows,

$$P^{\mathrm{b}}(v) = \int \frac{P(v)}{B(v)} d(v) = \int \frac{n V^s}{m V^r} d(v) \tag{5}$$

Integration of equation (5) yields the carbon-specific photosynthesis of organisms whose size ranges from v_0 to v_1:

$$P^{\mathrm{b}} = \frac{n/m}{1 + s - r} \left({v_1}^{1+s-r} - {v_0}^{1+s-r} \right) \tag{6}$$

This equation can be represented as a continuous function:

$$P^{\mathrm{b}} = \left(\frac{n}{m} \right) V_c^{(s-r)} \tag{7}$$

which contains the rate coefficient (n/m; intercept of the photosynthesis size spectrum divided by the intercept of the biomass size spectrum), the size scaling exponent ($s-r$; slope of the photosynthesis size spectrum minus the slope of the biomass size spectrum) and the cell volume (V_c) of the power function that defines the size spectrum of carbon-specific photosynthesis (i.e. $M = aW^b$, defined in Introduction).

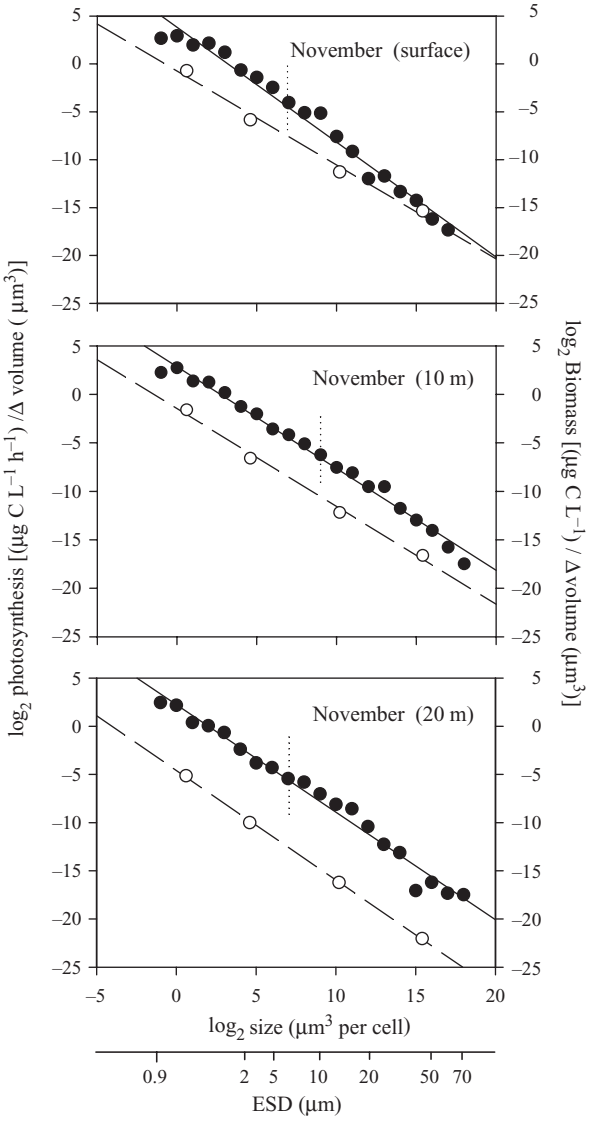

Fig. 1. Normalized biomass (solid circles) and metabolism (open circles) size spectra for phytoplankton assemblages at 0, 10 and 20 m depth in November 2001. Straight and dashed lines represent least square linear regression of the normalized biomass and metabolism size spectra, respectively. Phytoplankton size is represented as $\log_2$ cell volume and equivalent spherical diameter (ESD). Dotted line represents the limit of flow cytometry and image analysis subranges used to build up the whole phytoplankton spectra. Parameters for these regressions are given in Table I.

Additional methodological considerations

In order to elucidate whether four fractionation points (0.2, 2, 5 and 20 µm) for photosynthesis were sufficient to establish a continuous metabolism-size function, further analyses were required. We conducted several experiments which included additional fractionations (3 and 10 µm) within the phytoplankton size range. These analyses consistently showed that, in winter,

normalized spectra of photosynthesis followed the pattern described by the four-point functions used in this work, yielding determination coefficients (r^2) higher than 0.98 (Fig. 2). These results gave us confidence that our four-point based functions were not overlooking significant anomalies in the photosynthesis-size spectra during the period of study. In addition, we tested the reliability of the photosynthesis estimates from the continuous model by comparing them with the measurements of size-fractionated photosynthetic rates. Regression analysis (Model II) between estimates and measurements of size-fractionated photosynthetic rates ($n = 24$ for each size fraction) yielded slopes for the linear fit in the range 0.92–1.08, and determination coefficients in the range 0.82–0.95. For all size fractions, the intercept and slope of the linear fits were not significantly different from 0 and 1, respectively (*t*-test, $P > 0.05$).

Finally, it has to be borne in mind that the continuous biomass function overestimates systematically the biomass on the left-end side of the spectra, which represents the normally distributed populations of the smallest phytoplankton (<1.2 μm ESD). Thus, our analysis does not provide reliable estimates of carbon-specific photosynthesis below that cell size. For this reason, the size spectra of carbon-specific photosynthesis were constructed only for cell sizes >1.2 μm.

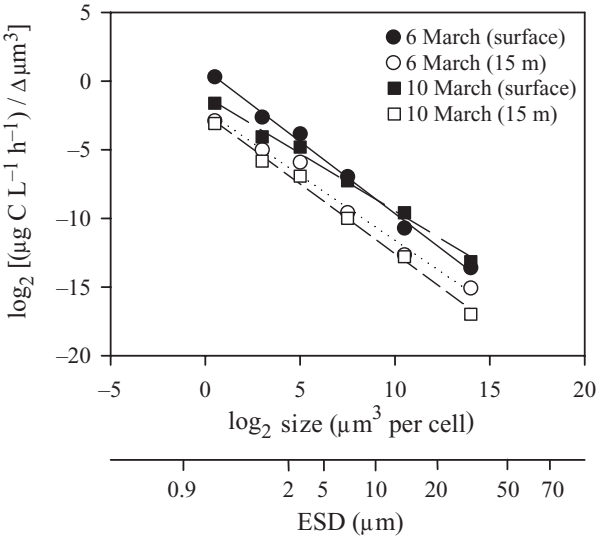

Fig. 2. Normalized metabolism size spectra composed by six fractionation points (0.2, 2, 3, 5, 10 and 20 μm) for phytoplankton assemblages in the Ría de Vigo. Lines represent least square linear regression. Solid line is for solid circles: $y = -1.05x + 0.8$ ($r^2 = 0.99$). Long-dashed line is for solid squares: $y = -0.95x–2.1$ ($r^2 = 0.99$). Dotted line is for open circles: $y = -0.84x–1.1$ ($r^2 = 0.98$). Short-dashed line is for open squares: $y = -1.02x–2.4$ ($r^2 = 0.99$). Phytoplankton size is represented as $\log_2$ cell volume and equivalent spherical diameter (ESD).

RESULTS

Hydrographic variability

The Ría de Vigo shows a marked degree of hydrographic seasonality, which strongly affects phytoplankton size structure. The temporal and vertical variability of temperature, nitrate concentration and photosynthetic rates from July 2001 to July 2002 have been described recently (Marañón *et al.*, 2004). From 5 November 2001 to 30 March 2002, we found vertical mixing. During this period, temperature varied between 12 and 16°C, and salinity ranged from 34.5 to 35.2. High nitrate concentrations (>4 μM) were measured throughout the water column. The 1% PAR level was located between 15 and 23 m. At the surface, Chl *a* concentration was in the range 0.6–1.7 mg m^{-3} and decreased with depth to values <0.6 mg m^{-3} at 20 m (Fig. 3). In general, the contribution of the different phytoplankton size classes to total Chl *a* was roughly similar and did not show significant changes with depth (Fig. 3). Using the Chl *a* measurements and estimates of phytoplankton C biomass, we also calculated the size-fractionated C:Chl *a* ratio. In general, we did not observe any differences in the C:Chl *a* ratio between depths. It is likely that the lack of vertical variability in the C:Chl *a* ratios was due to the continuous vertical mixing.

Biomass and photosynthesis size spectra

Normalized biomass spectra were used to characterize the phytoplankton size structure. Log_2-transformed spectra showed slopes ranging from −0.85 to −1.21 throughout the sampling period (Fig. 1, see Table I for power fits). A slope of −1 indicates that, in logarithmic size classes, biomass is equally distributed along the size spectrum. High spectral regularities were found throughout the study, as evidenced by the high determination coefficients ($r^2 > 0.92$). In spite of such regularity, a more detailed analysis revealed the existence of normally distributed subgroups underlying the overall biomass spectra. Fig. 4 shows the normalized biomass distribution of the different analytical populations (subgroups) during this study. We consistently observed that as cell size increases, the taxonomic composition varied from small cyanobacteria (i.e. *Synechococcus* sp.) and picoeukaryotes to cryptophytes and large diatoms.

The metabolism spectra, represented on a $\log_2$-scale by a linear function, yielded a slope which varied between −0.71 and −1.14 (Fig. 1, see Table I). In general, the numerical value of the slope decreased (i.e. became more negative) with depth, indicating a higher contribution of small-sized phytoplankton to the total community photosynthesis towards the base of the euphotic layer.

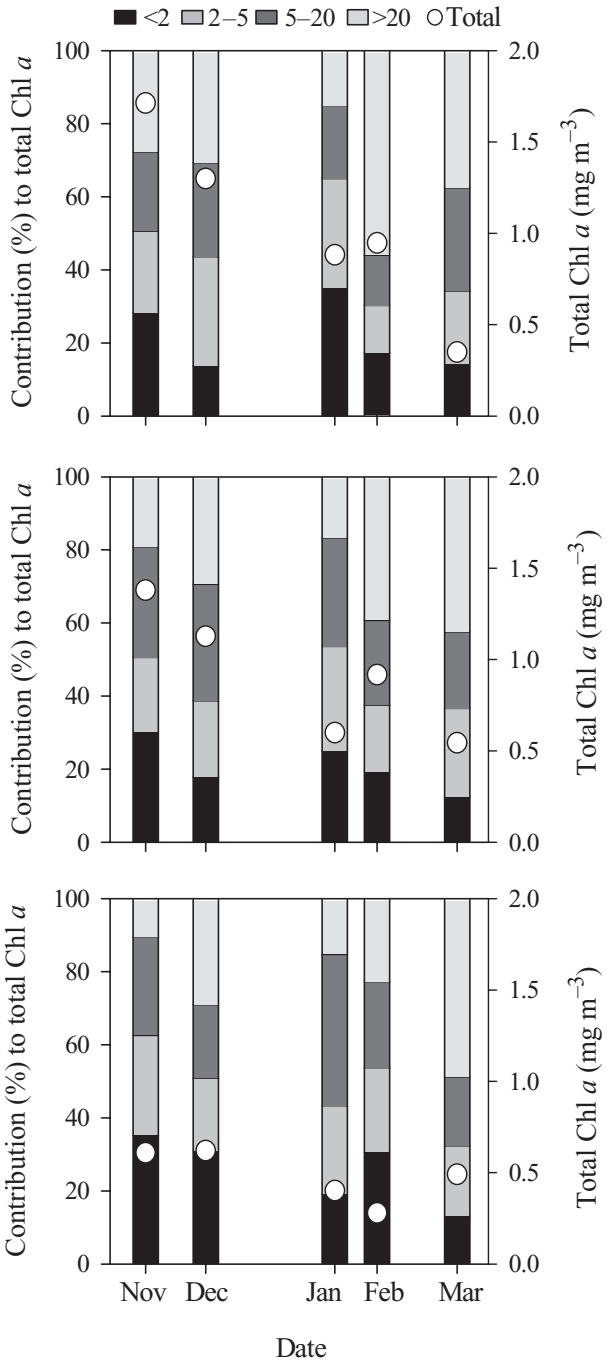

Fig. 3. Total Chl *a* concentration and the relative contribution (%) of picoplankton, small nanoplankton, large nanoplankton and microplankton to total Chl *a* by phytoplankton assemblages sampled from November 2001 to March 2002. Top, middle and bottom panels correspond to 0,10 and 20 m, respectively.

Carbon-specific photosynthesis size spectra

We modelled the size spectra of carbon-specific photosynthesis (P^b, equation 7) for the whole data set (Fig. 5, Table I). The slope of the P^b size spectrum, calculated from the model parameters, varied from −0.11 to 0.22. At the surface, the slope was positive, indicating that larger phytoplankton sustained higher rates of P^b than smaller cells. At the bottom of the euphotic layer the slopes were significantly lower than those measured at surface and 10-m depth (Kruskal–Wallis test, $P < 0.05$, Fig. 6). This means that under light-limited conditions, large-sized phytoplankton tend to sustain similar or lower growth rates than small-sized cells which might be related to the so called 'package effect' (Raven, 1998).

We also calculated the size-fractionated, Chl *a*-specific photosynthesis ($P^{\mathrm{Chl}\ a}$), an estimate of photosynthetic efficiency that to a certain extent can be compared to the carbon-specific photosynthesis (P^b). At the surface, $P^{\mathrm{Chl}\ a}$ increased consistently with increasing phytoplankton size. On average, the size-fractionated $P^{\mathrm{Chl}\ a}$ at surface were 2.9 ± 1.6, 2.2 ± 1.5, 4.6 ± 2.5 and 5.2 ± 2.4 mg C mg Chl a^{-1} h^{-1} for the <2, 2–5, 5–20 and >20 μm size fractions, respectively. At 20-m depth, $P^{\mathrm{Chl}\ a}$ decreased to values as low as 0.8 ± 0.1, 0.6 ± 0.2, 0.9 ± 0.3 and 0.3 ± 0.1 mg C mg Chl a^{-1} h^{-1} for the <2, 2–5, 5–20 and >20 μm size fractions, respectively. This decrease was much steeper in the large nanophytoplankton and microphytoplankton size classes. Thus, the patterns of size-fractionated $P^{\mathrm{Chl}\ a}$ are consistent with the slopes of the P^b size spectra. Importantly, the measurements of size-fractionated $P^{\mathrm{Chl}\ a}$ also indicate that, at the surface and 10-m depth, large-sized phytoplankton have higher photosynthetic efficiencies than smaller cells.

DISCUSSION

Physiological and ecological scaling factors

The size dependence of biomass-specific metabolic rates, such as photosynthesis and respiration, has been regarded as a major determinant of biological production in aquatic ecosystems (Platt et al., 1984). These allometric relationships have been recognized as a primary or physiological scaling factor in the analysis of pelagic ecosystems, which is consistent with a size scaling exponent of −0.25 for organism growth (Peters, 1983). Our biomass size spectra showed enough regularity so as to allow a continuous analysis of the biomass distribution patterns, by conforming the data set to a steady-state linear model as that described by Platt and Denman (Platt and Denman, 1978). In spite of such a regular spectra, a more detailed analysis revealed the existence of normally distributed subgroups underlying the overall biomass size spectra (Fig. 4). As cell size increased along the community size spectrum, parallel changes in the taxonomic composition were observed, from small cyano-

Table I: Parameters for power fits to the normalized biomass size-spectra [$B(v) = m\ V^r$], normalized photosynthesis size-spectra [$P(v) = n\ V^s$] and their derived P^b size spectra

Date	Depth (M)	$B(v)$	r^2	SE slope	$P(v)$	r^2	SE slope	P^b
05 November 2001	0	$14.3\ V^{-1.21a,b}$	0.98	0.04	$0.31\ V^{-0.99a}$	0.99	0.06	$0.09\ V^{0.22}$
	10	$7.27\ V^{-1.05a}$	0.99	0.03	$0.37\ V^{-1.01a}$	0.99	0.04	$0.05\ V^{0.04}$
	20	$4.73\ V^{-1.12a}$	0.98	0.01	$0.04\ V^{-1.14a}$	0.99	0.02	$0.01\ V^{-0.02}$
03 December 2001	0	$7.15\ V^{-1.09b}$	0.99	0.03	$0.22\ V^{-1.03}$	0.99	0.09	$0.03\ V^{0.06}$
	10	$4.52\ V^{-1.07}$	0.99	0.03	$0.31\ V^{-1.05}$	0.99	0.03	$0.07\ V^{0.02}$
	20	$1.26\ V^{-0.99}$	0.98	0.03	$0.01\ V^{-1.09}$	0.99	0.01	$0.01\ V^{-0.1}$
31 January 2002	0	$8.71\ V^{-1.14b}$	0.92	0.11	$0.49\ V^{-1.07}$	0.98	0.09	$0.06\ V^{0.07}$
	10	$3.51\ V^{-1.01}$	0.92	0.09	$0.17\ V^{-1.06}$	0.99	0.06	$0.05\ V^{-0.05}$
	20	$2.75\ V^{-1.02}$	0.95	0.06	$0.02\ V^{-1.13}$	0.99	0.05	$0.01\ V^{-0.11}$
18 February 2002	0	$7.43\ V^{-0.97b}$	0.98	0.03	$0.06\ V^{-0.84}$	0.99	0.09	$0.01\ V^{0.13}$
	10	$5.76\ V^{-0.98}$	0.98	0.03	$0.13\ V^{-0.91}$	0.99	0.09	$0.02\ V^{0.07}$
30 March 2002	0	$2.11\ V^{-0.93b}$	0.93	0.07	$0.03\ V^{-0.76}$	0.98	0.06	$0.01\ V^{0.17}$
	10	$1.03\ V^{-0.85}$	0.95	0.05	$0.02\ V^{-0.71}$	0.98	0.05	$0.02\ V^{0.14}$

The units of m and n are $(\mu m^3)^{-r}\ L^{-1}$ and $(\mu m^3)^{-s}\ L^{-1}\ h^{-1}$, respectively, thus $B(v)$ and $P(v)$ are in L^{-1} and $L^{-1}\ h^{-1}$, respectively, and P^b is in h^{-1}.
[a]Spectra shown in Fig. 1.
[b]Spectra shown in Fig. 4.

bacteria to large diatoms. An interesting approach to understanding this feature of size spectra has been proposed by Dickie *et al.* (Dickie *et al.*, 1987). They suggested that the community is scaled at two different levels according to primary and secondary scaling factors. The primary scaling factor corresponds with the global spectrum and represents the physiological constraints imposed by organism size. The secondary or ecological scaling factor accounts for the interspecific variability in growth efficiency as well as for possible interactions between organisms. This scaling factor is commonly assessed at the level of trophic group (i.e. phytoplankton and zooplankton). However, it can also be observed when analysing exclusively the phytoplankton size range. Size-differential grazing pressure may account for characteristic spectral shapes (Gaedke, 1993). In addition, group-specific growth efficiencies, related to different ecophysiological strategies to acquire and use resources for growth and maintenance, can also cause departures of the biomass spectra from the theoretical expectations. Although we did not determine the specific composition of the different subgroups, to a certain extent general taxonomic groups could be associated with them (Fig. 4). Variability in the specific composition along the community size spectrum appears to explain the fact that a weak size dependence of P^b may be observed when studying the phytoplankton community as a whole (Chisholm, 1992). Moreover, the phyletic diversity of the phytoplankton community introduces, through the numerical value of the rate coefficient (i.e. parameter a from equation $M = aW^b$, described in the Introduction), an important component of uncertainty in estimating the slope of the metabolism–size relationship. The numerical value of parameter a has been reported to change according to the metabolic strategy used by each organism group. Although an overall value has been proposed for all unicellular organisms (Peters, 1983), significant differences in this parameter have been observed between phytoplankton groups such as dinoflagellates and diatoms (see review by Chisholm, 1992). For example, diatoms grow faster than dinoflagellates of the same size. Thus, it is possible that interspecific differences in the rate coefficient may override the overall size dependence of community metabolism. This would account for observed deviations from the $^3/_4$-power rule of the size scaling exponent in natural phytoplankton communities.

Variability in the size scaling exponent of photosynthesis

The high variability in the size scaling of phytoplankton photosynthesis questions the applicability of the traditional size scaling metabolic exponents in predictive models of community metabolism. Our work suggests that this variability is likely due to changes in the phyletic composition across the phytoplankton size spectrum and also to changes in environmental conditions such as irradiance. The taxon-related variability has been previously addressed by Joint and Pomroy (Joint and Pomroy, 1988), who applied the allometric exponents proposed by Banse (Banse, 1982) for diatoms and dinoflagellates. However, our results suggest size scaling

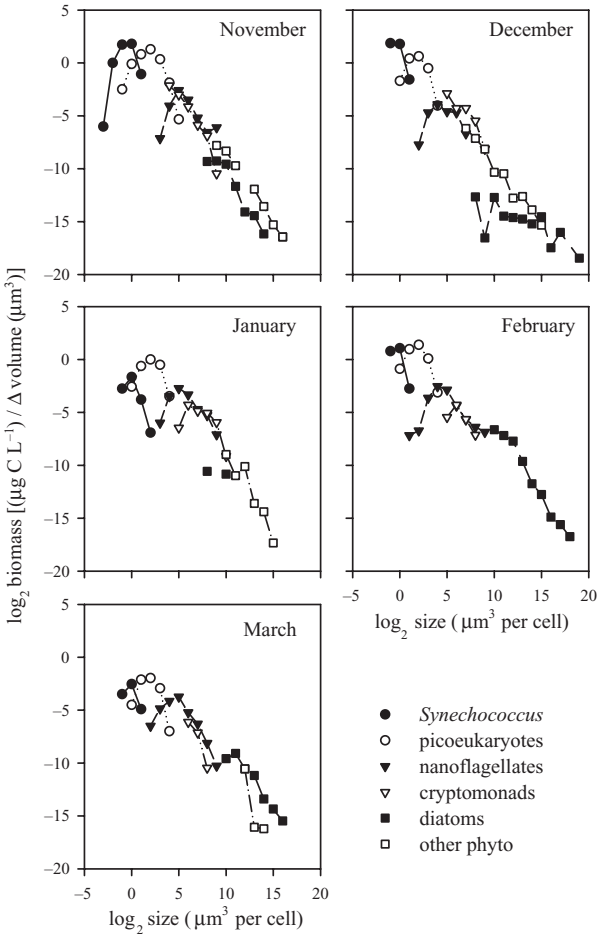

Fig. 4. Normalized biomass spectrum showing the different analytical populations (see text for details) observed at surface during each sampling day. Phytoplankton size is represented as $\log_2$ cell volume. Parameters for power fits to the overall normalized size spectrum are given in Table I.

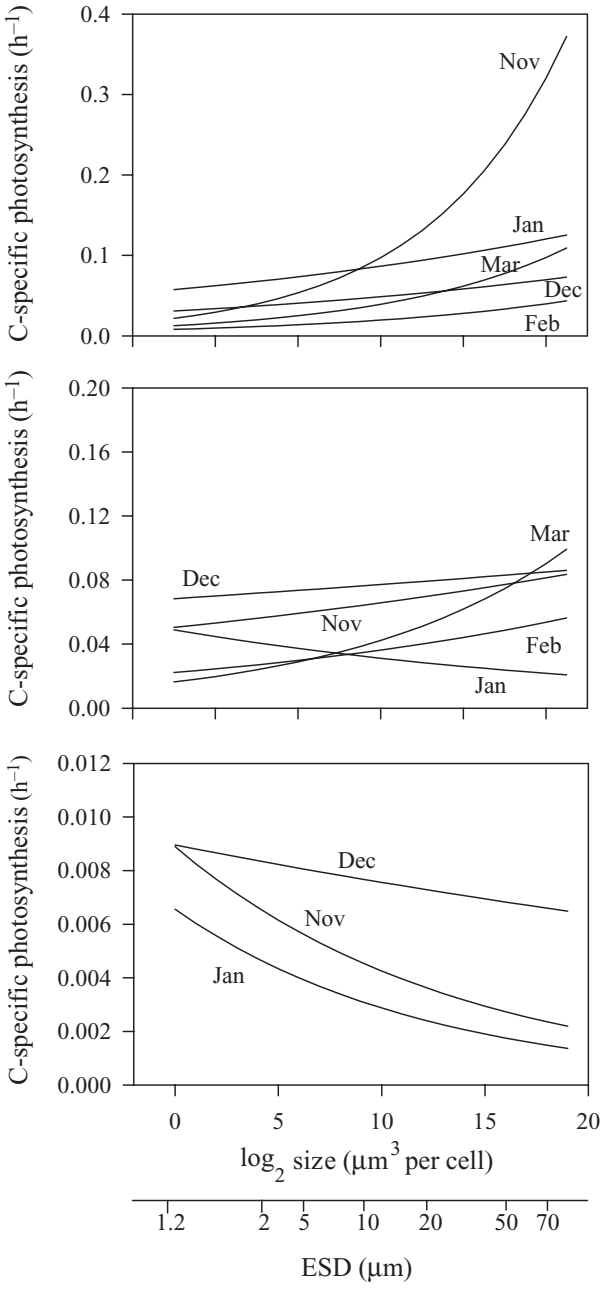

Fig. 5. Size spectra of biomass-specific photosynthesis for phytoplankton assemblages obtained from the model, P^b = (intercept metabolism spectrum/intercept biomass spectrum) × $V_{cell}^{(slope\ metabolism - slope\ biomass\ spectrum)}$. Phytoplankton size is represented as $\log_2$ cell volume and equivalent spherical diameter (ESD). Top, middle and bottom panels correspond to 0, 10 and 20 m, respectively.

relationships that are significantly different from those previously used and that, in addition, show a marked degree of variability.

We have shown that the slope of the P^b size spectrum may become positive. We would expect a positive size scaling in P^b to be associated with an increase in biomass stocks of large-sized phytoplankton, which however is not consistent with the observed slopes and regular structure of the biomass size spectra, as well as the patterns of size-fractionated Chl *a* obtained during our study. This discrepancy between the biomass and the metabolism size spectra may be explained by vertical mixing and lateral advection, which disperse phytoplankton assemblages throughout the water column and into adjacent ecosystems. In addition, higher sedimentation rates of larger cells may have also prevented them from accumulating in surface waters (Kiørboe, 1993; Tremblay and Legendre, 1994). In this regard, it is important to note that our metabolism spectra were constructed using instantaneous metabolic rates, whereas biomass spectra reflect a series of different mechanisms operating at larger scales. Most importantly, a positive slope of the P^b size spectrum has important implications for our understanding of

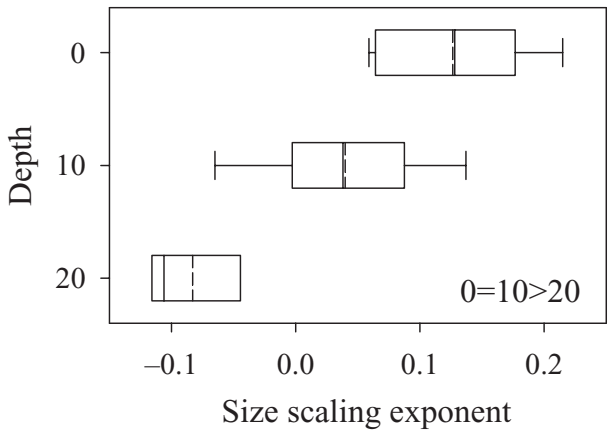

Fig. 6. Composite vertical distribution of the size scaling exponent of biomass-specific photosynthesis obtained from the five observations made from November 2001 to March 2002. Boxes enclose the 25 and 75% percentiles of the data, bars encompass 95% of the data, the central solid line represents the median and the central dashed line represents the mean. Significant differences between depths are indicated in the lower right corner of the panel.

phytoplankton dynamics in natural ecosystems. Standing stocks of small phytoplankton tend to be more strictly controlled by microzooplankton grazing, since both groups of organisms have roughly similar turnover rates. On the contrary, large phytoplankton and mesozooplankton, which have longer generation times than those of phytoplankton, may more likely to be uncoupled over temporal scales (Kiørboe, 1993). According to this view, the dominance of large phytoplankton in productive waters has been related to the uncoupling between large phytoplankton and mesozooplankton grazing (Banse, 1992). However, our observations of a positive slope of the P^b size spectrum provide another feasible explanation, purely based on phytoplankton physiology, for the dominance of large-sized phytoplankton in resource-rich environments.

In principle, our study does not strictly account for phytoplankton net metabolism, since this would require to obtain both photosynthesis and respiration estimates within the phytoplankton size range. This issue could be solved by knowing the size scaling of phytoplankton respiration. However, there exists a great uncertainty concerning how phytoplankton respiration changes with cell size (Finkel, 2001; Raven and Kübler, 2002). Banse (Banse, 1976) indicated that phytoplankton respiration is independent of cell size. In contrast, an exponent of −0.25 has been recently reported for marine diatoms cultured in laboratory (Finkel, 2001), suggesting that small phytoplankton have higher mass-specific respiration rates than larger phytoplankton. According to our results, a size scaling exponent of phytoplankton net metabolism of −0.25 would only be predicted if there was a greater carbon-specific loss of organic carbon from larger than from smaller cells. However, previous works appear to indicate the contrary (Laws, 1975; Raven, 1998; Finkel, 2001; see also Raven and Kübler, 2002). Thus, despite the fact that our results cannot be directly related to phytoplankton net metabolism, previous evidence on the size dependence of phytoplankton respiration support our conclusion that large phytoplankton may possess higher specific growth rates than smaller cells, at least under near-optimal resource conditions, namely high irradiance levels and nutrient concentrations.

Another possible source of bias in our photosynthesis measurements is the size-differential effect of zooplankton grazing. Although we do not have any data on grazing rates at our site, it is unlikely that grazing has affected our photosynthesis measurements in any way, because incubation time was short (2 h). Mesozooplankton are excluded from our experiments, due to the small size of the incubation bottles (80 ml). However, phytoplankton photosynthesis could be underestimated if significant losses of labelled carbon (^{14}C), due to microzooplankton grazing and subsequent respiration, take place during the incubation. The importance of these losses should decrease with decreasing incubation time, as the specific ^{14}C activity of the different organic carbon pools involved will be progressively smaller. It has to be taken into account that, for grazing activity to decrease the amount of ^{14}C in particulate matter, the ingested material needs to be respired during the course of the incubation. The model of Laws (Laws, 1984) allows a computation of the impact of grazing on ^{14}C-based estimates of photosynthesis. Taking the extreme instance of a phytoplankton assemblage growing at 2 d^{-1} and a grazing rate equal to 99% of phytoplankton growth, and assuming that microzooplankton lose 80% of the daily ingested carbon as respired CO_2, then herbivory during a 2-h incubation would cause a decrease of only 6% in the amount of particulate organic ^{14}C. These calculations and additional observations (e.g. Sakshaug *et al.*, 1997) strongly suggest that microzooplankton grazing does not cause a significant underestimation of photosynthetic rates as determined in short-term incubations with ^{14}C.

In conclusion, we have shown that the relationship between phytoplankton metabolism and cell size is highly variable. Under favourable conditions for growth, namely high irradiance and nutrient concentration, the slope of the P^b size spectrum may become positive. This finding represents an alternative possibility based on the physiological features of phytoplankton to account for the dominance of larger cells in resource-rich environments. We suggest that changes in the taxonomic composition along the size spectrum of phytoplankton communities (i.e. from small cyanobacteria to large diatoms) may be responsible

for such departure from the expected slope of −0.25. Along the vertical light gradient, the size-differential package effect might be implied in controlling the slope of the P^b size spectrum. Further work should be devoted to determine if the highly variable and, more importantly, positive size dependence of P^b in phytoplankton is a recurrent feature in other marine ecosystems.

ACKNOWLEDGEMENTS

We are grateful to F. Jiménez and L. Zabala for providing flow cytometry and microscopy image analysis. We also thank C. G. Castro for nutrient analysis and V. Pérez and P. Serret for their assistance in photosynthesis measurements. Kevin Flynn and three anonymous reviewers provided valuable comments that helped us to improve an earlier version of the manuscript. P.C. was supported by a postgraduate research fellowship from the Spanish Ministry of Science and Technology (MCYT). This research was funded by MCYT through research grant REN2000-1248 to E.M.

REFERENCES

Álvarez-Salgado, X. A., Figueiras, F. G., Pérez, F. F. *et al.* (2003) The Portugal coastal counter current off NW Spain: new insights on its biogeochemical variability. *Prog. Oceanogr.*, **56**, 281–321.

Banse, K. (1976) Rates of growth, respiration and photosynthesis of unicellular algae as related to cell size – a review. *J. Phycol.*, **12**, 135–140.

Banse, K. (1982) Cell Volumes, maximum growth rates of unicellular algae and ciliates, the role of ciliates in the marine pelagial. *Limnol. Oceanogr.*, **27**, 1059–1071.

Banse, K. (1992) Grazing, temporal changes of phytoplankton concentrations, and the microbial loop in the open sea. In Falkowski, P. G. and Woodhead, A. D. (eds), *Primary Productivity and Biogeochemical Cycles in the Sea.* Plenum Press, New York, pp. 409–440.

Blanco, J. M., Echevarría, F. and García, C. (1994) Dealing with size-spectra: some conceptual and mathematical problems. In Rodríguez, J. and Li, W. K. W. (eds), *The Size Structure and Metabolism of the Pelagic Ecosystem. Sci. Mar.*, **58**, 17–29.

Blanco, J. M., Quiñones, R. A., Guerrero, F. *et al.* (1998) The use of biomass spectra and allometric relations to estimate respiration of planktonic communities. *J. Plankton Res.*, **20**, 887–900.

Blasco, D., Packard, T. T. and Gardfield, P. C. (1982) Size dependence of growth rate, respiratory electron transport system activity, and chemical composition in marine diatoms in the laboratory. *J. Phycol.*, **18**, 58–63.

Chisholm, S. W. (1992) Phytoplankton size. In Falkowski, P. G. and Woodhead, A. D. (eds), *Primary Productivity and Biogeochemical Cycles in the Sea.* Plenum Press, New York, pp. 213–237.

Dickie, L. M., Kerr, S. R. and Boudreau, P. R. (1987) Size-dependent processes underlying regularities in the ecosystem structure. *Ecol. Monogr.*, **57**, 233–250.

Duplisea, D. E. and Kerr, S. R. (1995) Application of a biomass size spectrum to demersal fish data from the Scotian Shelf. *J. Theor. Biol.*, **177**, 263–269.

Fenchel, T. (1974) Intrinsic rate of natural increase: the relationship with body size. *Oecologia*, **14**, 317–326.

Finkel, Z. V. (2001) Light absorption and size scaling of light-limited metabolism in marine diatoms. *Limnol. Oceanogr.*, **46**, 86–94.

Finkel, Z. V., Irwin, A. J. and Schofield, O. (2004) Resource limitation alters the $^3/_4$ size scaling of metabolic rates in phytoplankton. *Mar. Ecol. Prog. Ser.*, **273**, 269–279.

Gaedke, U. (1993) Ecosystem analysis based on biomass distributions: a case study of a plankton community in a large lake. *Limnol. Oceanogr.*, **38**, 112–127.

Gasol, J. M., Guerrero, R. and Pedrós-Alió, C. (1991) Seasonal variations in size structure and prokaryotic dominance in sulfurous Lake Cisó. *Limnol. Oceanogr.*, **36**, 860–872.

Grasshoff, K., Kremling, M. and Ehrdardt, M. (1999) *Methods of Seawater Analysis*, 3rd edn. Wiley-VCH, Weinheim.

Hemmingsen, A. M. (1960) Energy metabolism as related to body size and respiratory surfaces, and its evolution. *Rep. Steno Mem. Hosp.*, **9**, 15–22.

Joint, I. R. and Pomroy, A. J. (1988) Allometric estimation of the productivity of phytoplankton assemblages. *Mar. Ecol. Prog. Ser.*, **47**, 161–168.

Kiørboe, T. (1993) Turbulence, phytoplankton cell size and the structure of pelagic food webs. *Adv. Mar. Biol.*, **29**, 1–72.

Laws, E. A. (1975) The importance of respiration losses in controlling the size distribution of marine phytoplankton. *Ecology*, **56**, 419–426.

Laws, E. A. (1984) Improved estimates of phytoplankton carbon based on ^{14}C incorporation into chlorophyll *a*. *J. Theor. Biol.*, **110**, 425–434.

Marañón, E., Cermeño, P., Fernández, E. *et al.* (2004) Significance and mechanisms of photosynthetic production of dissolved organic carbon in a coastal eutrophic ecosystem. *Limnol. Oceanogr.*, **49**, 1652–1666.

Nielsen, S. L. and Sand-Jensen, K. (1990) Allometric scaling of maximum photosynthetic growth rate to surface/Volume ratio. *Limnol. Oceanogr.*, **35**, 177–181.

Peters, R. H. (1983) *The Ecological Implications of Body Size.* Cambridge University Press, Cambridge.

Platt, T. and Denman, K. (1978) The structure of pelagic ecosystems. *Rapp. p.-v. Reun. Cons. Perm. Int. Explor. Mer.*, **173**, 60–65.

Platt, T., Lewis, M. and Geider, R. (1984) Thermodynamics of the pelagic ecosystem: elemental closure conditions for biological production in the open ocean. In Fasham, M. J. R. (ed.), *Flows of Energy and Material in Marine Ecosystems.* Plenum Press, New York and London, pp. 49–84.

Quiñones, R. A. (1992) Size distribution of planktonic biomass and metabolic activity in the pelagic ecosystem. PhD Thesis. University of Dalhouise, Canada.

Quiñones, R. A. (1994) A comment on the use of allometry in the study of pelagic ecosystem processes. In Rodríguez, J. and Li, W. K. W. (eds.), *The Size Structure and Metabolism of the Pelagic Ecosystem., Sci. Mar.*, **58**, 11–16.

Quiñones, R. A., Blanco, J. M., Echevarría, F., Fernández-Puelles, M. L., Gilabert, J., Rodríguez, V. and Valdés, L. (1994) Metabolic size spectra at a frontal station in the Alborán Sea. In Rodríguez, J. and Li, W. K. W. (eds.), *The Size Structure and Metabolism of the Pelagic Ecosystem. Sci. Mar.*, **58**, 53–58.

Quiñones, R. A., Platt, T. and Rodríguez, J. (2003) Patterns of biomass-size spectra from oligotrophic waters of the Northwest Atlantic. *Prog. Oceanogr.*, **57**, 405–427.

Raven, J. A. (1998) Small is beautiful: the picophytoplankton. *Funct. Ecol.*, **12**, 503–513.

Raven, J. A. and Kübler, J. E. (2002) New light on the scaling of metabolic rate with the size of algae. *J. Phycol.*, **38**, 11–16.

Rodríguez, J. (1994) Some comments on the size-based structural analysis of the pelagic ecosystem. *Sci. Mar.*, **58**, 1–10.

Rodríguez, J., Blanco, J. M., Jiménez-Gómez, F. *et al.* (1998) Patterns in the size structure of the phytoplankton community in the deep fluorescence maximum of the Alboran Sea (southwestern Mediterranean). *Deep-Sea Res. I*, **45**, 1577–1593.

Rodríguez, J., Jiménez, F., Bautista, B. *et al.* (1987) Planktonic biomass spectra dynamics during a winter production pulse in Mediterranean coastal waters. *J. Plankton Res.*, **9**, 1183–1194.

Rodríguez, J., Jiménez-Gómez, F., Blanco, J. M. *et al.* (2002) Physical gradients and spatial variability of the size structure and composition of phytoplankton in the Gerlache Strait (Antarctica). *Deep-Sea Res. II*, **49**, 693–706.

Rodríguez, J. and Mullin, M. M. (1986) Relation between biomass and body weight of plankton in a steady-state ecosystem. *Limnol. Oceanogr.*, **31**, 361–370.

Ruiz, J., García, C. M. and Rodríguez, J. (1996) Sedimentation loss of phytoplankton cells from the mixed layer: effects of turbulence levels. *J. Plankton Res.*, **18**, 1727–1734.

Sakshaug, E., Bricaud, A., Dandonneau, Y. *et al.* (1997) Parameters of photosynthesis: definitions, theory and interpretation of results. *J. Plankton Res.*, **19**, 1637–1670.

Schlesinger, D. A., Molot, L. A. and Shuter, B. J. (1981) Specific growth rates of freshwater algae in relation to cell size and light intensity. *Can. J. Fish. Aquat. Sci.*, **38**, 1052–1058.

Sommer, U. (1989) Maximal growth rates of Antarctic phytoplankton: only a weak dependence on cell size. *Limnol. Oceanogr.*, **34**, 1109–1112.

Sprules, W. G. and Munawar, M. (1986) Plankton size spectra in relation to ecosystem productivity, size, and perturbation. *Can. J. Fish. Aquat. Sci.*, **43**, 1789–1794.

Tang, E. P. Y. (1995) The allometry of algal growth rates. *J. Plankton Res.*, **17**, 1325–1335.

Thiebaux, M. L. and Dickie, L. M. (1993) Structure of the body-size spectrum of the biomass in aquatic ecosystems: a consequence of the allometry in predator–prey interactions. *Can. J. Fish. Aquat. Sci.*, **50**, 1308–1317.

Tremblay, J. E. and Legendre, L. (1994) A model for the size-fractionated biomass and production of marine phytoplankton. *Limnol. Oceanogr.*, **39**, 2004–2014.

Valulot, D., Courties, C., Partensky, F. (1989) A simple method to preserve oceanic phytoplankton for flow cytometry analysis. In Yentsch, C. M. and Horan P. K. (eds), *Cytometry in aguatic sciences. Cytometry*. **10**, pp 629–635.

Verity, P. G., Robertson, C. Y., Tronzo, C. R. *et al.* (1992) Relationships between cell Volume and the carbon and nitrogen content of marine photosynthetic nanoplankton. *Limnol. Oceanogr.*, **37**, 1434–1446.